HHS Public Access

Author manuscript

Stem Cells. Author manuscript; available in PMC 2016 March 07.

Published in final edited form as:

Stem Cells. 2015 August ; 33(8): 2596–2612. doi:10.1002/stem.2044.

Cannabinoid Receptor-2 Regulates Embryonic Hematopoietic Stem Cell Development via Prostaglandin E2 and P-Selectin Activity

Virginie Esain[a], **Wanda Kwan**[a], **Kelli J. Carroll**[a], **Mauricio Cortes**[a], **Sarah Y. Liu**[a], **Gregory M. Frechette**[a], **Lea M. V. Sheward**[a], **Sahar Nissim**[b,c,d], **Wolfram Goessling**[b,c,d,e], and **Trista E. North**[a,e]

[a]Department of Pathology, Beth Israel Deaconess Medical Center, Harvard Medical School, Boston, Massachusetts, USA

[b]Division of Genetics, Brigham and Women's Hospital, Harvard Medical School, Boston, Massachusetts, USA

[c]Division of Gastroenterology, Brigham and Women's Hospital, Harvard Medical School, Boston, Massachusetts, USA

[d]Dana-Farber Cancer Institute, Harvard Medical School, Boston, Massachusetts, USA

[e]Harvard Stem Cell Institute, Cambridge, Massachusetts, USA

Abstract

Cannabinoids (CB) modulate adult hematopoietic stem and progenitor cell (HSPCs) function, however, impact on the production, expansion, or migration of embryonic HSCs is currently uncharacterized. Here, using chemical and genetic approaches targeting CB-signaling in zebrafish, we show that CB receptor (CNR) 2, but not CNR1, regulates embryonic HSC development. During HSC specification in the aorta-gonad-mesonephros (AGM) region, CNR2 stimulation by AM1241 increased *runx1;cmyb*$^{+}$ HSPCs, through heightened proliferation, whereas CNR2 antagonism decreased HSPC number; FACS analysis and absolute HSC counts confirmed and quantified these effects. Epistatic investigations showed AM1241 significantly upregulated PGE2 synthesis in a Ptgs2-dependent manner to increase AGM HSCs. During the phases of HSC production and colonization of secondary niches, AM1241 accelerated migration to the caudal hematopoietic tissue (CHT), the site of embryonic HSC expansion, and the thymus; however these effects occurred independently of PGE2. Using a candidate approach for HSC migration and retention factors, P-selectin was identified as the functional target of CNR2 regulation. Epistatic analyses confirmed migration of HSCs into the CHT and thymus was dependent on CNR2-

Correspondence: Trista E. North, Ph.D., Department of Pathology, Beth Israel Deaconess Medical Center, Center for Life Sciences 638, 3 Blackfan Circle, Boston, Massachusetts 02115, USA. Telephone: +1 (617) 735 2083; Fax: +1 (617) 735 2480; tnorth@bidmc.harvard.edu.

Author Contributions V.E.,W.K., K.J.C., G.M.F., S.Y.L., and L.V.S.: performed embryo exposures, MO injections, qPCR, and in situ hybridizations; V.E., W.K., M.C., and S.N.: conducted FACS, biochemical assays, IHC, Western and fluorescence microscopy; V.E., W.G., and T.E.N.: designed experiments and evaluated results; V.E. and T.E.N.: wrote the manuscript. All authors reviewed and edited the manuscript.

Disclosure of Potential Conflicts of Interest The authors indicate no potential conflicts of interest.

regulated P-selectin activity. Together, these data suggest CNR2-signaling optimizes the production, expansion, and migration of embryonic HSCs by modulating multiple downstream signaling pathways.

Keywords

Hematopoietic stem cells; Cell migration; Cannabinoids; Prostaglandin E2; Zebrafish; Proliferation

Introduction

In vertebrates, definitive hematopoietic stem cells (HSCs) give rise to all mature blood cell lineages throughout an individual's lifetime. Embryonic and adult HSCs interact with specialized microenvironments, or niches, which are required for their function [1]. HSCs dynamically respond to environmental cues to expand, differentiate, or inhabit the bone marrow (BM) niche. HSC mobilization and homing are tightly regulated by chemoattractants and adhesion molecules that are co-opted in therapeutic applications, such as HSC transplantation [2]; identifying regulatory components of each HSC niche is critical to improve efficiency of HSC therapies.

The transcription factor Runx1 is required for HSC development across vertebrates [3–5], where it functions in endothelial-to-hematopoietic transition (EHT) [6]. In zebrafish, *runx1*-expressing HSCs emerge from hemogenic endothelium in the aorta-gonad mesonephros (AGM) region around 30 hours post-fertilization (hpf) [7, 8], upregulating expression of *cmyb* and *cd41* after EHT [9, 10]. At 32–34 hpf, HSCs migrate to the caudal hematopoietic tissue (CHT), an intermediate site of hematopoiesis, to expand or differentiate, then migrate to seed the kidney marrow (KM) and thymus beginning at 48–60 hpf [9, 10]. Although embryonic HSC migration routes are well-described in zebrafish [9–11], the molecular mechanisms underlying HSC maturation remain elusive, including the rationale for successive niches and functional redundancies ensuring adequate HSC production.

In mammalian embryos, HSCs exhibit a maturation-dependent expression profile of adhesion molecules and chemokines thought to reflect their ability to colonize subsequent hematopoietic organs [12]. In the mouse, adhesion molecules including Cadherins, Integrins, and E-/P-Selectins are associated with migration to the fetal liver (FL) and BM [12], while thymic homing is regulated by chemokines [13, 14]. Adhesion molecules physically control migration through endothelium and extracellular matrix (ECM) [15], while chemokines and cytokines regulate hematopoietic stem and progenitor cell (HSPC) movements by establishing directional gradients [15, 16]: for example, CXCR4/CXCL12 (Stromal-Derived Factor (SDF)-1) interactions are crucial for HSC transit from FL to the BM and thymus [12, 13, 17, 18] and BM retention. Shifting hematopoietic niches during ontogeny may enable proper HSC maturation via exposure to these differential microenvironmental signals [1]. Concomitant with HSC induction and migration, there is a rapid expansion such that between E12.5 and E14.5 murine FL HSCs double in number [19]. Zebrafish HSCs similarly expand in the CHT [11], although precise proliferation rates are not established [20–22]. Hypoxia-Inducible Factor 1-alpha (HIF1α), Insulin-like Growth Factor (IGFs),

Wnts, and prostaglandin E2 (PGE2) each influence adult HSC proliferation in vivo and in vitro [23], as well as HSC expansion during development [24–28]. Several factors regulating BM retention and HSC migration likewise regulate cell proliferation [29–32], but additional roles in embryonic HSC production, expansion, or differentiation remain undetermined.

Eicosanoids are a family of lipid modifiers related to arachidonic acid (AA) that includes: epoxyeicosatrienoic acids, leukotrienes, prostaglandins, and endocannabinoids (eCBs). Several are known modifiers of adult HSC function [33], and their synthesis/signaling pathways are highly interconnected. During zebrafish development, PGE2 modulates Wnt-signaling to control HSC production, while in adult fish or mice, it enhances hematopoietic regeneration after injury [25, 28], through increased HSC proliferation and CXCR4-mediated homing [34, 35]. eCBs 2-arachidonoylglycerol (2-AG) and anandamide (AEA) similarly modulate cell proliferation and migration of mammalian hematopoietic cells in vitro [36–42]. Endogenous and synthetic CBs bind to G-protein coupled receptors: CNR1, CNR2, and GPR55 [43]. While in humans, CNR2 is predominantly expressed on immune cells [44], both CNR1 and CNR2 are expressed on murine and human HSCs [33]. In the mouse, CNR2-signaling increases recovery after irradiation by modifying HSPC proliferation and apoptosis [45]; furthermore, CNR2-agonists can mobilize Colony-Forming Unit Granulocyte Macrophage (CFU-GM) into peripheral blood and enhance the effect of Granulocyte-Colony Stimulating Factor (G-CSF) [45]. While CNR2-signaling modifies multiple aspects of adult HSPC behavior, its impact on embryonic HSC formation, expansion, or hematopoietic niche colonization is unknown.

Here, we demonstrate a role for CBs during zebrafish hematopoiesis. Embryonic exposure to eCBs or CNR2-selective agonists increases *runx1*$^{+}$ HSPCs. Using discrete treatment intervals, we show AM1241-mediated CNR2-stimulation during hemogenic niche specification (18–24 hpf) enhances AGM HSC development, while treatment during the window of HSC production (30–36 hpf) and colonization (30–96 hpf) alters HSPC number in subsequent niches, the CHT and thymus. AM1241 exposure increases PGE2 synthesis and signaling via prostaglandin endoperoxide synthase 2 (Ptgs2) upregulation. In contrast, the impact of CNR2-stimulation on HSPC expansion and niche migration is PGE2-independent, requiring the P-selectin pathway; loss of P-selectin function disrupts CHT and thymic homing and blocks the stimulatory effect of CNR2-signaling. Together, these data reveal a novel role for CBs during vertebrate definitive hematopoiesis.

Materials and Methods

Zebrafish Husbandry

Zebrafish were maintained according to IACUC-approved protocols. Tg(*-6.0itga2b(CD41):eGFP*) [46], Tg(*kdrl(flk1):eGFP*) [47], Tg(*CD45:dsRed*) [9], Tg(*kdrl(flk1):dsRed2*) [48], Tg(*lmo2:dsRed*) [49], Tg(*cmyb:eGFP*) [28], Tg(*runx1P2:eGFP*) [50], and Tg(*rag2:GFP*) [51] lines were described previously.

Chemical Treatments and Evaluation

Zebrafish embryos were exposed to compound modifiers (Supporting Information Table 1) in E3 water in multiwell plates for durations noted. Whole-mount in situ hybridization (WISH) was performed as previously described [26]. Qualitative phenotypes for individual embryos ($n \geq 25$ embryos per condition, ≥3 replicates) were scored as relatively high/medium/low in expression compared to sibling controls and graphically depicted as the percentage falling into each of the three phenotypic expression bins; “medium” expression was set as the most representative phenotype in the normal bell-curve distribution of each cohort of control embryos per experiment. For immunohistochemistry (IHC), embryos were fixed in 4% paraformaldehyde (PFA) and dehydrated overnight (O/N) in MeOH at −20°C. After rehydration and Phosphate Buffered Saline (PBS)/0.1% Tween20 (PBT) washes, embryos were incubated in prechilled acetone (−20°C (20 minutes)) and rinsed in dH_2O before proteinase K digestion (10 μg/mL (6–12 minutes)). Primary antibodies (Supporting Information Table 2) were incubated O/N in Block (PBT, 2% Bovine Serum Albumine (BSA), 2% sheep serum), before secondary antibody staining (RT (2 hours)). Statistical significance was determined by Student's *t* test, as indicated.

Morpholino Injection

Morpholino (MOs) (Supporting Information Table 3, GeneTools) were injected as described previously [52].

Microscopy

Fluorescent embryos were treated as above and imaged as previously described [28]. For IHC, embryos were mounted in Fluoromount-G (Southern Biotech) and imaged using Zeiss LSM510 Meta 2-Photon or 700 Laser Scanning Confocal Microscopes. Cell counts and thymic area were quantified using ImageJ (NIH).

Flow Cytometry and Fluorescence Activated Cell Sorting

Endothelial cells (Flk1:dsRed$^+$;cMyb:GFP$^-$) and HSCs (Flk1: dsRed$^+$;cMyb:GFP$^+$) were sorted from *flk1:dsRed;cmyb:GFP* double positive transgenic embryos at 48 hpf. After cell collection, RNA was extracted, treated with DNaseI (RNAqueous-Micro Total RNA isolation Kit, Life Technologies, Rockville, MD, http://www.lifetech.com) and amplified with Ovation RNA Amplification System V2 (NuGEN). Flow cytometric analysis of HSCs was previously detailed [28].

Quantitative Reverse Transcriptase Polymerase Chain Reaction

Quantitative polymerase chain reaction (qPCR) was performed on cDNA isolated from pooled embryos and/or fluorescence-activated cell sorted (FACS) isolated subsets at time points indicated ($n = 25$ embryos per variable; primers: Supporting Information Table 4) using ABI PRISM 7900HT (Invitrogen, Carlsbad, CA, http://www.invitrogen.com). Ct values were determined using PCR Miner [53] and fold-change calculated by the ΔΔCt or R0 method with *tbp* or *18s* as the reference gene.

Western Blot and PGE2 Metabolite Measurements

Western blot analysis (Supporting Information Table 3) was conducted on pooled embryo lysates as described [26] ($n \geq 50$ embryos per condition), repeated in triplicate and quantified using ImageJ (NIH). PGE2 metabolite measurements were performed according to manufacturer's protocols (Cayman Chemical) on pooled embryo lysates ($n = 30$ embryos per condition) following compound incubation (5 μM [12–24 hpf]).

Results

CNR2-Signaling Positively Regulates AGM HSC Development

PGE2 modulates HSC development and homeostasis in vertebrates [28]. To determine if related eicosanoids similarly impact embryonic HSC production and function, we assessed effects of endogenous and synthetic CBs. Embryonic exposure to endogenous ligands 2-AG and AEA during the onset of hematopoiesis (12–30 hpf), increased AGM *runx1* expression, as determined by WISH (Fig. 1A, 1C); O2545, a CNR1/CNR2-agonist, elicited a similar response (Fig. 1C; Supporting Information Fig. S1A). Whereas the CNR1-agonist arachidonyl-2-chloroethylamide (ACEA) exhibited no effect on *runx1* (Fig. 1C; Supporting Information Fig. S1A), CNR2-agonists AM1241 (Fig. 1A, 1C) and JWH015 (Supporting Information Fig. S1E, S1F) recapitulated the eCB phenotype. The effect of AM1241 was quantified by qPCR, revealing significantly increased *runx1* and *cmyb* expression at 36 hpf (Supporting Information Fig. S1C). Similarly, absolute cell counts of Flk1:dsRed^{+};cMyb:GFP^{+} (yellow) AGM HSCs [54] revealed a significant enhancement following eCB exposure, due to CNR2-selective stimulation (Fig. 1B, 1D; Supporting Information Fig. S1B). *cnr2* was expressed throughout the embryo from 18–48 hpf, with strong AGM expression at 24 hpf (Fig. 1E and data not shown). qPCR of FACS-sorted fractions of *flk1:dsRed;cmyb:GFP* transgenic embryos confirmed *cnr2* expression in the Flk1:dsRed^{+};cMyb:GFP^{+} double positive HSC population (Supporting Information Fig. S1D). To examine functional requirements, *cnr1* and *cnr2* were knocked-down using modified antisense oligonucleotides (MO). While *cnr1*-MO had no effect, *cnr2*-morphants exhibited reduced *runx1* expression at 30 hpf (Fig. 1F, 1G) and significantly decreased Flk1:dsRed^{+};cMyb:GFP^{+} HSCs at 36 hpf (Fig. 1H, 1I); *cnr2*-MO also blocked AM1241-mediated induction of *runx1* expression, confirming receptor selectivity (Supporting Information Fig. S1G, S1H). Similar inhibitory effects were found for the CNR2-antagonist AM630 (Supporting Information Fig. S1I, S1J). These data show CNR2-signaling positively modulates HSC number during the onset of embryonic definitive hematopoiesis.

CNR2-Stimulation Regulates HSPC Development in Distinct Hematopoietic Niches

Embryonic HSC development can be divided into four broad, partially overlapping phases: (a) hematopoietic niche specification (18–24 hpf); (b) AGM HSC production (30–48 hpf); (c) CHT colonization and HSC expansion (34–72 hpf) [10, 11, 55]; and (d) KM and thymus colonization (>2.5–5 dpf) [9, 10] (Supporting Information Fig. S2A). AM1241-treatment during niche specification (18–24 hpf) increased AGM *runx1/cmyb* levels at 30 hpf (Fig. 2A, 2B), which was confirmed by evaluation of Runx1P2:eGFP expression (Supporting Information Fig. S2B) and quantified by whole-embryo HSPC FACS using *cmyb:eGFP;lmo2:dsRed* embryos (Supporting Information Fig. S2C). Absolute counts of

double positive Flk1:dsRed^{+};cMyb:GFP^{+} HSCs within the AGM corroborated the expansion observed following CNR2-stimulation (Fig. 2C, 2D). In contrast, exposure to AM630 during niche specification significantly decreased, but did not eliminate, *runx1* expression (Fig. 2A, 2B) or Flk1:dsRed^{+};cMyb:GFP^{+} HSC production (Fig. 2C, 2D), indicating eCBs are not essential for hemogenic induction but actively modulate HSC numbers.

Embryos exposed to AM1241 during HSC production (30–38 hpf) had no appreciable change in AGM *runx1;cmyb* expression (Supporting Information Fig. S2D), however, CHT localization was strongly increased (Fig. 2E, 2F). This finding was confirmed by CD41:GFP^{+} HSC enumeration in the CHT [26] (Fig. 2G, 2H). 3-hour interval time-course analysis documented the transition from HSPC production in the AGM to initiation of CHT colonization (27–42 hpf) in the presence and absence of CNR2-modulation (Fig. 2I, 2J; Supporting Information Fig. S2E) In wild type (WT) embryos, *runx1;cmyb* expression was present in the CHT starting at 30 hpf; while the onset of colonization was not affected by CNR2-stimulation, elevated *runx1;cmyb* expression was found in the CHT of AM1241-treated embryos at all times from 30–39 hpf, suggesting CNR2-signaling accelerates colonization. AM630-treatment during HSC production likewise caused no alterations in *runx1;cmyb* expression (Fig. 2E, 2F) or CD41:GFP^{+} HSCs at the onset of CHT colonization (Fig. 2G, 2H), however, defects were noted as time progressed, such that by 48 hpf significantly fewer CHT HSCs were present (Fig. 2K; Supporting Information Fig. S2F). These data suggest CNR2 influences the rate of CHT migration for newly produced HSCs.

To further assess the role of CNR2-signaling in colonization of secondary hematopoietic niches, HSPCs were evaluated at 4 dpf when adult hematopoietic organs are actively seeded. AM1241-treatment increased total *cmyb* expression at 4 dpf by qPCR analysis (Fig. 3B); however, CHT HSPCs were not grossly altered (Fig. 3A). Whereas, *cmyb* expression in the KM was also indistinguishable from controls, localization of *cmyb*^{1} progenitors in the thymus was robustly increased by AM1241 (Fig. 3A, 3C), implying CNR2-signaling may selectively modulate embryonic thymic homing; markers of T-cell differentiation, *rag2* and *lck*, were likewise increased (Fig. 3D–3G). Image analysis revealed significant expansion in thymic *rag2* expression in AM1241-exposed embryos (Fig. 3H, 3I), and qPCR showed increased expression of the lymphoid progenitor marker *ikaros* (Fig. 3L). To better characterize the apparent increase in lymphoid-specific colonization, the dynamics of *ikaros* and *rag1* expression in the thymus was examined from 60 to 96 hpf. CNR2-stimulation did not alter the onset of *ikaros* (Fig. 3J; Supporting Information Fig. S3A) or *rag1* expression (Fig. 3K) but rather increased expression levels per embryo compared to controls at all time points. In contrast, following treatment from 30 to 96 hpf, AM630 markedly decreased thymic *cmyb*, *rag1*, and *lck* staining (Fig. 3A–3I); however, reduced *cmyb*$^{+}$ HSPCs were also noted in the CHT, indicating loss of CNR2-signaling may impact HSPC expansion (Fig. 3A). In sum, CNR2-signaling maintained a role in HSPC production and migration throughout embryogenesis.

CNR2- and PGE2-Signaling Pathways Interact via Ptgs2 to Modulate HSPCs

We have previously shown that moderate elevations in PGE2 increase HSC formation in the AGM; as eicosanoid synthesis and signaling pathways are known to be interconnected [56], we next explored if CBs and PGE2 coordinately and/or redundantly regulated embryonic HSC formation. Consistent with prior observations [28], targeting PGE2 production by exposure to Prostaglandin endoperoxide synthase 1 (Ptgs1; SC-560) or Ptgs2 (NS-398) selective-inhibitors from 12 to 30 hpf decreased *runx1* expression (Fig. 4A, 4B). Cotreatment with AM1241 restored *runx1* expression to WT levels in SC-560- but not NS-398-exposed embryos; this effect was mimicked by MO-mediated knockdown of *ptgs1* and *ptgs2* as well as incubation with alternative selective inhibitors (Fig. 4C; Supporting Information Fig. S4A). Flk1:dsRed^{+};cMyb:eGFP^{+} cell counts in the AGM confirmed that coincubation with AM1241 rescued low HSC production in SC-560- but not NS-398-exposed embryos (Fig. 4D), suggesting Ptgs2-mediated PGE2 production was responsible for the effect of AM1241 on HSCs.

Both endogenous and synthetic CBs can modulate the transcription or activity of Ptgs2 [57–64] to regulate production of PGE2 from available AA, in a context-dependent manner. To test whether AM1241 impacted intraembryonic PGE2 levels, we measured PGE2-metabolite concentrations. PGE2-treated embryos showed increased PGE2-metabolites (2.66-fold), as expected; exposure to AM1241 also significantly (1.35-fold) enriched PGE2-metabolites (Fig. 4E). At 24 hpf, *ptgs1* was robustly expressed throughout the embryo, including the vasculature, consistent with previous reports [65]; in contrast, both *ptgs2* isoforms were more weakly expressed (Fig. 4F). Following AM1241-treatment, expression of each *ptgs* was visibly increased. qPCR indicated whereas *ptgs1* expression was not statistically increased over baseline levels, both *ptgs2a* and *ptgs2b* were significantly upregulated in response to CNR2-stimulation (Fig. 4G); CNR2-modulation also altered Ptgs2 protein levels compared to controls as indicated by Western blot (AM1241: 2.86-fold, AM630: 0.43-fold, Supporting Information Fig. S4B). To confirm that CNR2-signaling was responsible for *ptgs2* upregulation and subsequent PGE2-induced increases in HSPC production, modified epistasis experiments were performed: in addition to effects on *runx1* expression (Supporting Information Fig. S1G, S1H), MO-mediated inhibition of CNR2-signaling reduced the effect of AM1241 on *ptgs2* expression (Fig. 4F). Furthermore, reintroduction of *ptgs2b* mRNA returned *runx1* expression to baseline levels in the *cnr2* morphants (Fig. 4H, 4I). Additionally, knockdown of prostaglandin E synthase (*ptges*) (Supporting Information Fig. S4C) or that of the PGE2-receptors: *ptger2a/b* and *4a/b* (Supporting Information Fig. S4D) antagonized the effect of AM1241 on *runx1* expression, demonstrating PGE2 production and downstream signaling was necessary for AGM HSPC regulation. Finally, combinatorial treatment with AM1241 and PGE2 increased the percentage of embryos with high *runx1*$^{+}$ expression, particularly at suboptimal doses incapable of affecting HSC production alone (Supporting Information Fig. S4E, S4F), which was confirmed by CD41:eGFP^{+};CD45:dsRed^{+} FACS at 36 hpf (Fig. 4J). Together, these data indicate increased PGE2 production resulting from transcriptional upregulation of *ptgs2* via AM1241-stimulation enhances AGM HSC production.

AM1241-Mediated Increases in PGE2 Affect Only AGM HSC Expansion

To determine if functional interactions between CNR2- and PGE2-signaling in HSC regulation occurred throughout embryogenesis, embryos were exposed to AM1241 with or without NS-398 for discrete intervals. AM1241-exposure during hemogenic endothelial specification failed to increase AGM *runx1* expression with simultaneous NS-398 treatment (Fig. 5A, 5B), which was confirmed by enumeration of Flk1:dsRed^{+};cMyb:GFP^{+} HSCs at 36 hpf (Fig. 5E; Supporting Information Fig. S5A). In contrast, during HSC production and CHT colonization, NS-398 had no effect on AM1241-mediated increases in *runx1*;*cmyb*$^{+}$ localization or expansion (Fig. 5C, 5D), as was corroborated by CD41:GFP^{+} cell counts in the CHT at 38 hpf (Fig. 5F; Supporting Information Fig. S5B). Furthermore, during niche specification, H89-treatment, inhibiting Protein Kinase A (PKA) activity downstream of PGE2-receptor stimulation [25], diminished *runx1* expression, reduced Flk1:dsRed^{+};cMyb:GFP^{+} AGM HSCs (Fig. 5A, 5B, 5E; Supporting Information Fig. S5A), and blocked the effect of AM1241-exposure. In contrast, H89-treatment during HSC production and CHT colonization did not disrupt AM1241-mediated increases in *runx1*;*cmyb* or CD41:GFP^{+} HSCs in the CHT (Fig. 5C, 5D, 5F; Supporting Information Fig. S5B). CNR2 can signal through the modulation of multiple downstream effectors [66]. To determine which signaling cascade(s) were impacted by CNR2 modulation, Western blot analysis was performed on embryos exposed to AM1241 and AM630 during niche specification or HSC production. Following CNR2-modulation from 18 to 24 hpf, phospho-ERK (pERK) levels were increased 1.55-fold by AM1241 and reduced 0.49-fold with AM630 treatment, however phospho-AKT (pAKT) levels were unaffected (Supporting Information Fig. S5C and data not shown). In contrast, when treatment occurred during HSC production (30–38 hpf), AM1241 and AM630 were observed to modulate pAKT levels (AM1241: 1.79-fold, AM630: 0.63-fold), but not pERK signaling (Supporting Information Fig. S5D and data not shown), mirroring the differential impact on PGE2 activity occurring during HSC formation.

PGE2 affects hemogenic niche development as well as HSC proliferation in zebrafish, mice, and humans [25, 28, 34, 65]; CNR2 agonists similarly regulate hematopoietic cell proliferation and survival in adult mice [28, 45] and human cell lines [67]. To further characterize the mechanism of CNR2-stimulated HSC production, vascular development and proliferation were assessed. Neither *flk1:GFP* expression was impacted by AM1241 nor were markers of vessel identity: *efnb2a* and *flt4* (Supporting Information Fig. S5E–S5G). Early AM1241 treatment (18–24 hpf) increased proliferation within the Flk1:GFP^{+} dorsal aorta of the AGM region at 30 hpf (Fig. 5G, 5H), as delineated by phospho-histone H3 (pH3, red) staining; NS-398 decreased pH3^{+} AGM cells and blocked the effect of AM1241, consistent with PGE2-mediated HSC regulation. In contrast, while later AM1241 exposure (30–38 hpf) also enhanced the number of proliferating (blue) cMyb:GFP^{+} HSPCs within Flk1:dsRed^{+} vessels of the CHT (Fig. 5I, 5J) at 38 hpf, Ptgs2 inhibition had no effect on the proproliferative response to AM1241. In sum, PGE2 production and downstream activities are necessary for AM1241-augmented AGM HSC formation; however, enhanced CHT colonization and HSPC expansion are independent of PGE2.

The Effect of AM1241 on CHT Colonization Is Mediated by P-selectin

PGE2 increases homing of mammalian adult HSCs to the BM [34, 35]; CNR2-signaling also modulates adult hematopoietic migration [33, 36–42, 68]. As AM1241-mediated effects on CHT colonization were independent of PGE2, we sought to identify hematopoietic adhesion and migration factors differentially regulated by each eicosanoid. Although PGE2 and CNR2-agonists have opposite effects on CXCL12/CXCR4 expression in vitro [35, 69], both *cxcr4b* and *cxcl12b* were significantly upregulated following embryonic AM1241- or PGE2-treatment (Supporting Information Fig. S6A). MMP9 also exhibits opposing responses to PGE2- and CNR2-signaling in murine dendritic cells [70, 71]; however, while dmPGE2 increased embryonic *mmp9* expression, it was unchanged by AM1241, making it an unlikely candidate for CNR2-stimulated CHT colonization (Supporting Information Fig. S6A). Epistatic experiments using AMD3100 (CXCR4 antagonist) and SB-3CT (MMP2/9 inhibitor), as well as *cxcr4/cxcl12* knockdown studies, confirmed the expression analysis and eliminated each pathway as causal for the CNR2-mediated colonization phenotype (Supporting Information Fig. S6B and data not shown).

We next assessed adhesion factors expressed in the vasculature of the developing zebrafish embryo from the Cadherin, Protocadherin, and Integrin families (Supporting Information Fig. S6C–S6E): by qPCR, no statistically differential regulation was observed between PGE2- or AM1241-treatment. Conversely, while *e-selectin* (*sele*) showed no statistical difference, both *p-selectin* (*selp*) and *p-selectin glycoprotein ligand-1* (*psgl-1*) expression were significantly upregulated at 36 hpf by AM1241, but not PGE2 (Fig. 6A). *selp* and its ligand, *psgl-1*, are expressed in the vasculature from 18 to 72 hpf [72, 73]. qPCR analysis of *psgl-1*, *selp*, and *sele* expression on FACS-sorted endothelial cells (Flk1:dsRed^{+};cMyb:GFP^{-}) and HSCs (Flk1:dsRed^{+};cMyb:GFP^{+}) revealed *psgl-1* is predominantly expressed on HSCs, *selp* is only detected in endothelial cells, and *sele* is in both fractions (Fig. 6B; Supporting Information Fig. S6F). At 38 hpf, *runx1*;*cmyb* expression in the CHT was decreased following *selp* or *psgl-1* knockdown (Fig. 6C, 6D); moreover, in morphant embryos, AM1241-exposure no longer impacted CHT colonization (Fig. 6C, 6D), as confirmed by CD41:eGFP analysis (Fig. 6E, 6F). To further validate the role of P-selectin, embryos were treated with KF38789, a selective inhibitor of P-selectin-mediated cell adhesion [74]; CD41:eGFP^{+} cell counts showed that KF38789 also caused reduced CHT colonization, particularly in AM1241-treated embryos (Fig. 6G, 6H). These data indicated CNR2-signaling modulates HSC colonization of the CHT through upregulation of P-selectin activity.

Colonization of the Thymus is Controlled by CNR2/P-Selectin-Signaling

We next sought to determine if P-selectin activity was likewise involved in CNR2-stimulated thymic colonization. qPCR analysis at 72 hpf indicated AM1241-exposure continued to significantly upregulate *psgl-1* and *selp*, but not *sele* (Fig. 6I). MO-mediated knockdown of *selp* and *psgl-1* decreased the appearance of *cmyb*$^{+}$ thymic HSPCs, and *rag1*-expressing lymphoid progenitors compared to controls (Fig. 7A–7D). Likewise, while total *cmyb* expression increased following CNR2-stimulation from 30 to 96 hpf, AM1241 failed to influence thymic colonization, or the appearance of *rag1*-expressing progenitors in *p-selectin* morphants (Fig. 7A–7D). Quantification Rag2:GFP^{+} expression at 96 hpf confirmed

p-selectin knockdown impaired thymic homing in WT embryos and reduced the effect of CNR2-stimulation (Fig. 7E, 7F); KF38789 (30–96 hpf) treatment replicated the morphant colonization phenotypes, strongly antagonizing the effect of AM1241 (Fig. 7G; Supporting Information Fig. S7F). Notably, qPCR analysis indicated *p-selectin* knockdown did not reduce total *cmyb* expression in AM1241-treated (30–96 hpf) embryos (Supporting Information Fig. S7C); WISH analysis confirmed morphant embryos displayed accumulated HSPCs in the CHT region (Supporting Information Fig. S7A, S7B) and/or increased *cmyb*$^+$ cells dispersed throughout the circulation (Supporting Information Fig. S7A, S7B); these phenotypes were similar, but exaggerated, after AM1241-treatment. However, based on *mpo* expression, elevation in circulating *cmyb*$^+$ cells was not indicative of biased commitment to the myeloid lineage (Supporting Information Fig. S7D). As CHT HSPC numbers were reduced by P-selectin antagonism at 38 hpf, but elevated at 96 hpf, time course analysis was performed: while CD41:GFP$^+$ cells remained slightly depressed in morphants at 48 hpf, loss of P-selectin activity led to significant accumulations in the CHT by 72 hpf, which remained present at 96 hpf (Supporting Information Fig. S7E). This data suggested that once HSPCs colonize the CHT they can expand normally but fail or delay in their ability to exit the CHT and/or colonize the thymus in the absence of P-selectin.

To determine if CNR2-signaling was required for P-selectin function during thymic colonization, embryos were exposed to AM630 following the completion of AGM HSC production and CHT seeding (48–96 hpf). Exposure to AM630 decreased *selp* expression at 96 hpf, but not that of *psgl-1*, indicating CNR2-signaling predominantly controls the rate-limiting component of P-selectin function (Fig. 7H). As seen in P-selectin morphants, AM630-treated embryos displayed increased numbers of CD41:GFP$^+$ cells in the CHT at 96 hpf (Fig. 7I; Supporting Information Fig. S7H), and reductions in lymphoid progenitors as assessed by thymic *ikaros* expression (Supporting Information Fig. S7I) and Rag2:GFP$^+$ fluorescence (Fig. 7J; Supporting Information Fig. S7G). Altogether, these data indicate CNR2-signaling regulates P-selectin activity during hematopoiesis to draw HSPCs to appropriate niches for expansion (CHT) and differentiation (thymus) during embryogenesis.

Discussion

HSC specification and production from hemogenic endothelium is a complex and multistep process, requiring the combined and sequential action of multiple pathways [75]. The mechanisms underlying subsequent colonization movements which allow HSC maturation, expansion, and homing to adult hematopoietic sites are less well-characterized, but likely require niche-supplied cytokines, ECM-modifiers, and adhesion molecules [1]. These processes are exquisitely timed and regulated to ensure sufficient numbers of mature HSCs, while simultaneously allowing the onset of differentiation into various effector lineages; as such, hematopoiesis must invoke overlapping, even redundant pathways, with mechanisms for feedback and cross-regulatory control to achieve appropriate balance. Here, we demonstrate CNR2-signaling modifies HSC production and proliferation within the AGM, as well as colonization of CHT and thymus; however, we also discovered hematopoiesis continues, albeit less effectively, in its absence. Our data indicate CNR2-signaling is a biologically relevant modifier of the multistep HSC development process, potentiating effects of other known, and perhaps also unknown, primary regulators.

Eicosanoids have emerged as potent modulators of HSC formation and function in adult vertebrates [28, 33, 35, 45]. eCBs are known to modify cell proliferation and migration of murine [36, 41, 42] and human [37–40, 67] hematopoietic cells in vitro. In humans, CNR2 is predominantly expressed on adult immune cells [44], including immunophenotypically defined HSCs [33]. In mice, CNR2-signaling modulates HSC proliferation and survival, as well as mobilization from the BM niche [33, 45]. Here, we revealed novel roles for CNR2-signaling in vivo during embryogenesis, impacting several aspects of HSPC development. Interestingly, CNR2-deficient mice have no gross morphologic alterations but exhibit a decreased number of specialized B-, T-, and natural killer cells. A similar blood phenotype has not been directly reported in CNR2$^{-/-}$ embryos, however our data suggests that inability to properly seed the thymus may underlie this adult observation, which warrants additional targeted investigation in the developmental setting. In zebrafish, while CNR2-stimulation during AGM specification increased HSCs by enhancing PGE2 levels, AM1241-treatment during HSC production instead accelerated colonization and expansion of mature HSCs in the CHT, and later, thymic progenitors, via the P-selectin pathway. The pleiotropy of effects that CNR2-signaling exerts on HSC function is likely to impact different biological processes in hematopoietic progenitors and immune effector cells, and as such, may be responsible for the presence of both anti-inflammatory and proinflammatory outcomes from CNR2 stimulation on murine models of infection and autoimmune disease [76].

In human and mouse, factors regulating BM mobilization and retention, such as CXCR4/CXCL12 and E-/P-Selectin, can affect cell proliferation [29–32]. Our attempt to determine if HSC elevation following CNR2-stimulation was a consequence of earlier arrival of HSCs in the CHT, allowing more time to expand, or a direct proproliferative effect on HSCs, was complicated by the fact that both functions are contemporaneous. However, observations of *cmyb*$^{+}$ and CD41:GFP^{+} cells stranded in the CHT, or scattered throughout the embryo, argue in favor of a more significant role for CNR2-signaling in colonization of secondary niches, rather than cell proliferation per se, implying proproliferative effects are simply a consequence of earlier arrival or late departure of progenitors.

While often considered directly opposing actions, HSC mobilization and homing or retention are not mirror images, but different processes involving overlapping and distinct mechanisms [77]. Here, we show CNR2-modulation, through P-selectin, affects HSC migration from the AGM to CHT, and CHT to thymus, but not to the KM, suggesting its role is more complex than simply stimulating egress. In the mouse, P-selectin influences homing of adult lymphoid progenitors to the thymus by modulating extravasation from the blood vessels [78], consistent with our observations of embryonic *selp* and *psgl-1* expression in zebrafish. P-selectin is present on murine thymic endothelium [78], and PSGL-1 expression is gradually upregulated as HSCs mature [79], however, mechanisms controlling seeding of the embryonic thymus, including requirements for P-selectin function, remain to be definitively established [13, 14, 17, 80, 81]. CNR1 and CNR2 are highly expressed in fetal murine thymus [82]; however, in contrast to our data, perinatal exposure to Δ_9-THC caused profound thymic atrophy and T-cell apoptosis [82]. This discrepancy may stem from the fact that we examined an earlier subpopulation, included within the CD4^{+}/CD8^{+} fraction, but not later thymocytic stages [82]. Alternatively, enhanced colonization in our

assays may be specific to direct activation of CNR2, as plant-derived CBs often exhibit a higher affinity for CNR1. In vitro, CNR2-stimulation promotes or inhibits T-cell migration and proliferation depending on both agonist- and dose-selection [76], perhaps highlighting the context-dependent role of CNR2 as a modifier, rather than required, HSPC regulator.

The interplay between bioactive lipids—which can derive from common precursors, intraconvert, and transcriptionally activate enzymatic machinery for related pathways—is a relatively underappreciated mechanism to modulate individual regulatory outcomes in a tissue-specific manner; one might speculate that such interactions could explain the pleiotropic effect of CNR2-signaling on HSC development. PGE2 is an established regulator of HSCs across vertebrate species and a promising therapeutic candidate [83]; here, we show CNR2-signaling directly modulates PGE2 production via Ptgs2 to increase embryonic HSCs. Effects of CB-signaling on P-selectin remain controversial, as its ability to modulate *P-selectin*/*PSGL-1* expression varies depending on the model [53, 84–88]; these discrepancies could also reflect an indirect mechanism of CB regulation. In mouse, thymic levels of the bioactive phospholipid S1P vary in parallel to that of P-selectin [89], and S1P regulates lymphocyte trafficking [90] as well as HSC mobilization similarly to CNR2 [91]. CB- and S1P- signaling interact at multiple levels: AEA increases S1P phosphorylation [92], and CNR1-stimulation enhances ceramide biosynthesis, the substrate for S1P [93, 94]; further, sphingosine can bind to CNR1 as an antagonist [95], suggesting potential feedback regulation. It will be interesting to determine if just as CNR2-signaling modulates AGM HSCs through cross-regulatory effects on PGE2; CHT and thymus colonization occurs via regulation of S1P or other lipid mediators.

Demand-driven hematopoiesis, initiated by inflammatory feedback loops, is well-characterized to stimulate HSC mobilization, proliferation, and differentiation to provide an adequate response to infection or injury. In the adult, HSCs and more committed downstream progenitors, express receptors for most of the proinflammatory molecules [96], however, a similar role for these factors during embryogenesis is not as well-established. Factors within this class, such as PGE2 [25, 28] and nitric oxide [52], as well as more recently type I and II interferons [97, 98], TNFα [99] and TLR4-MyD88-NF-κB pathway [100], were shown by our lab and others to be active in the embryo and necessary for the proper HSC development; the data presented here reveal a novel role for CNR2-signaling as a modifier of HSC production and function during embryogenesis, acting via inflammatory modulation.

Conclusion

In summary, this study provides direct evidence that CNR2 signaling regulates HSC emergence and movement to the subsequent hematopoietic niches, the CHT and the thymus. While in the AGM, CB/CNR2 signaling enhances PGE2 synthesis via the up-regulation of Ptgs2 impacting HSC production; in contrast, CNR2 stimulation promotes subsequent niche colonization by increasing P-selectin signaling. Our work indicates that CB/CNR2 activity acts as a modifier of embryonic HSC formation by fine-tuning signaling pathways essential for HSC emergence and colonization of secondary niches.

Supplementary Material

Refer to Web version on PubMed Central for supplementary material.

Acknowledgments

We thank P. Crosier and K. Crosier (University of Auckland) for *runx1P2:eGFP* fish, D. Traver (*UCSD*) for the *CD45:dsRed* line, and K. Poss (Duke University) for *flk1:dsRed* transgenics. We also thank Daniel Tenen and Kristin K. Brown (BIDMC) for advices on cannabinoid signaling and the Western blot analysis, respectively. FACS analyses were conducted with assistance from the BIDMC/HSCI FACS Core. This investigation was supported by the Philippe Foundation (V.E.) and the NIDDK: K01DK080226 and R03DK096156-01 (T.E.N.).

References

1. Cao H, Oteiza A, Nilsson SK. Understanding the role of the microenvironment during definitive hemopoietic development. Exp Hematol. 2013; 41:761–768. [PubMed: 23800491]
2. Thomas ED, Lochte HL Jr, Lu WC, et al. Intravenous infusion of bone marrow in patients receiving radiation and chemotherapy. N Engl J Med. 1957; 257:491–496. [PubMed: 13464965]
3. North TE, de Bruijn MFTR, Stacy T, et al. Runx1 expression marks long-term repopulating hematopoietic stem cells in the midgestation mouse embryo. Immunity. 2002; 16:661–672. [PubMed: 12049718]
4. North T, Gu TL, Stacy T, et al. Cbfa2 is required for the formation of intra-aortic hematopoietic clusters. Development. 1999; 126:2563–2575. [PubMed: 10226014]
5. Orkin SH, Zon LI. Hematopoiesis: An evolving paradigm for stem cell biology. Cell. 2008; 132:631–644. [PubMed: 18295580]
6. Chen MJ, Yokomizo T, Zeigler BM, et al. Runx1 is required for the endothelial to haematopoietic cell transition but not thereafter. Nature. 2009; 457:887–891. [PubMed: 19129762]
7. Kalev-Zylinska ML, Horsfield JA, Flores MVC, et al. Runx1 is required for zebrafish blood and vessel development and expression of a human RUNX1-CBF2T1 transgene advances a model for studies of leukemogenesis. Development. 2002; 129:2015–2030. [PubMed: 11934867]
8. Burns CE, DeBlasio T, Zhou Y, et al. Isolation and characterization of runxa and runxb, zebrafish members of the runt family of transcriptional regulators. Exp Hematol. 2002; 30:1381–1389. [PubMed: 12482499]
9. Bertrand JY, Kim AD, Teng S, et al. CD41+ cmyb+ precursors colonize the zebrafish pronephros by a novel migration route to initiate adult hematopoiesis. Development. 2008; 135:1853–1862. [PubMed: 18417622]
10. Kissa K, Murayama E, Zapata A, et al. Live imaging of emerging hematopoietic stem cells and early thymus colonization. Blood. 2008; 111:1147–1156. [PubMed: 17934068]
11. Murayama E, Kissa K, Zapata A, et al. Tracing hematopoietic precursor migration to successive hematopoietic organs during zebrafish development. Immunity. 2006; 25:963–975. [PubMed: 17157041]
12. Ciriza J, Hall D, Lu A, et al. Single-cell analysis of murine long-term hematopoietic stem cells reveals distinct patterns of gene expression during fetal migration. Plos One. 2012; 7:e30542. [PubMed: 22276210]
13. Calderón L, Boehm T. Three chemokine receptors cooperatively regulate homing of hematopoietic progenitors to the embryonic mouse thymus. Proc Natl Acad Sci USA. 2011; 108:7517–7522. [PubMed: 21502490]
14. Liu C, Ueno T, Kuse S, et al. The role of CCL21 in recruitment of T-precursor cells to fetal thymi. Blood. 2005; 105:31–39. [PubMed: 15358618]
15. Sahin AO, Buitenhuis M. Molecular mechanisms underlying adhesion and migration of hematopoietic stem cells. Cell Adhes Migrat. 2012; 6:39–48.
16. Ciriza J, Thompson H, Petrosian R, et al. The migration of hematopoietic progenitors from the fetal liver to the fetal bone marrow: Lessons learned and possible clinical applications. Exp Hematol. 2013; 41:411–423. [PubMed: 23395775]

17. Bleul CC, Boehm T. Chemokines define distinct microenvironments in the developing thymus. Eur J Immunol. 2000; 30:3371–3379. [PubMed: 11093154]
18. Ciriza J, García-Ojeda ME. Expression of migration-related genes is progressively upregulated in murine Lineage-Sca-1+c-Kit+ population from the fetal to adult stages of development. Stem Cell Res Ther. 2010; 1:14. [PubMed: 20637061]
19. Morrison SJ, Hemmati HD, Wandycz AM, et al. The purification and characterization of fetal liver hematopoietic stem cells. Proc Natl Acad Sci USA. 1995; 92:10302–10306. [PubMed: 7479772]
20. Alghisi E, Distel M, Malagola M, et al. Targeting oncogene expression to endothelial cells induces proliferation of the myeloerythroid lineage by repressing the notch pathway. Leukemia. 2013; 27:2229–2241. [PubMed: 23625115]
21. Hirabayashi R, Hozumi S, Higashijima S-I, et al. Ddx46 is required for multi-lineage differentiation of hematopoietic stem cells in zebrafish. Stem Cells Dev. 2013; 22:2532–2542. [PubMed: 23635340]
22. Li X, Lan Y, Xu J, et al. SUMO1-activating enzyme subunit 1 is essential for the survival of hematopoietic stem/progenitor cells in zebrafish. Development. 2012; 139:4321–4329. [PubMed: 23132242]
23. Walasek MA, van Os R, de Haan G. Hematopoietic stem cell expansion: Challenges and opportunities. Ann N Y Acad Sci. 2012; 1266:138–150. [PubMed: 22901265]
24. Austin TW, Solar GP, Ziegler FC, et al. A role for the Wnt gene family in hematopoiesis: Expansion of multilineage progenitor cells. Blood. 1997; 89:3624–3635. [PubMed: 9160667]
25. Goessling W, North TE, Loewer S, et al. Genetic interaction of PGE2 and Wnt signaling regulates developmental specification of stem cells and regeneration. Cell. 2009; 136:1136–1147. [PubMed: 19303855]
26. Harris JM, Esain V, Frechette GM, et al. Glucose metabolism impacts the spatiotemporal onset and magnitude of HSC induction in vivo. Blood. 2013; 121:2483–2493. [PubMed: 23341543]
27. Luis TC, Weerkamp F, Naber BAE, et al. Wnt3a deficiency irreversibly impairs hematopoietic stem cell self-renewal and leads to defects in progenitor cell differentiation. Blood. 2009; 113:546–554. [PubMed: 18832654]
28. North TE, Goessling W, Walkley CR, et al. Prostaglandin E2 regulates vertebrate haematopoietic stem cell homeostasis. Nature. 2007; 447:1007–1011. [PubMed: 17581586]
29. Eto T, Winkler I, Purton LE, et al. Contrasting effects of P-selectin and E-selectin on the differentiation of murine hematopoietic progenitor cells. Exp Hematol. 2005; 33:232–242. [PubMed: 15676218]
30. Lévesque J-P, Zannettino AC, Pudney M, et al. PSGL-1-mediated adhesion of human hematopoietic progenitors to P-selectin results in suppression of hematopoiesis. Immunity. 1999; 11:369–378. [PubMed: 10514015]
31. Mo W, Chen J, Patel A, et al. CXCR4/CXCL12 mediate autocrine cell- cycle progression in NF1-associated malignant peripheral nerve sheath tumors. Cell. 2013; 152:1077–1090. [PubMed: 23434321]
32. Winkler IG, Barbier V, Nowlan B, et al. Vascular niche E-selectin regulates hematopoietic stem cell dormancy, self renewal and chemoresistance. Nat Med. 2012; 18:1651–1657. [PubMed: 23086476]
33. Hoggatt J, Pelus LM. Eicosanoid regulation of hematopoiesis and hematopoietic stem and progenitor trafficking. Leukemia. 2010; 24:1993–2002. [PubMed: 20882043]
34. Goessling W, Allen RS, Guan X, et al. Prostaglandin E2 enhances human cord blood stem cell xenotransplants and shows long-term safety in preclinical nonhuman primate transplant models. Cell Stem Cell. 2011; 8:445–458. [PubMed: 21474107]
35. Hoggatt J, Singh P, Sampath J, et al. Prostaglandin E2 enhances hematopoietic stem cell homing, survival, and proliferation. Blood. 2009; 113:5444–5455. [PubMed: 19324903]
36. Jorda MA, Verkabel SE, Valk PJ, et al. Hematopoietic cells expressing the peripheral cannabinoid receptor migrate in response to the endocannabinoid 2-arachidonoylglycerol. Blood. 2002; 99:2786–2793. [PubMed: 11929767]

37. Joseph J, Niggemann B, Zaenker KS, et al. Anandamide is an endogenous inhibitor for the migration of tumor cells and T lymphocytes. Cancer Immunol Immunother. 2004; 53:723–728. [PubMed: 15034673]
38. Kishimoto S, Muramatsu M, Gokoh M, et al. Endogenous cannabinoid receptor ligand induces the migration of human natural killer cells. J Biochem. 2005; 137:217–223. [PubMed: 15749836]
39. Kishimoto S, Oka S, Gokoh M, et al. Chemotaxis of human peripheral blood eosinophils to 2-arachidonoylglycerol: Comparison with other eosinophil chemoattractants. Int Arch Allergy Immunol. 2006; 140(suppl 1):3–7. [PubMed: 16772720]
40. Oka S, Ikeda S, Kishimoto S, et al. 2-arachidonoylglycerol, an endogenous cannabinoid receptor ligand, induces the migration of EoL-1 human eosinophilic leukemia cells and human peripheral blood eosinophils. J Leukoc Biol. 2004; 76:1002–1009. [PubMed: 15316028]
41. Valk PJ, Delwel R. The peripheral cannabinoid receptor, Cb2, in retrovirally-induced leukemic transformation and normal hematopoiesis. Leuk Lymphoma. 1998; 32:29–43. [PubMed: 10036999]
42. Valk P, Verbakel S, Vankan Y, et al. Anandamide, a natural ligand for the peripheral cannabinoid receptor is a novel synergistic growth factor for hematopoietic cells. Blood. 1997; 90:1448–1457. [PubMed: 9269762]
43. Pertwee RG, Howlett AC, Abood ME, et al. International Union of Basic and Clinical Pharmacology. LXXIX. Cannabinoid receptors and their ligands: Beyond CB1 and CB2. Pharmacol Rev. 2010; 62:588–631. [PubMed: 21079038]
44. Galiègue S, Mary S, Marchand J, et al. Expression of central and peripheral cannabinoid receptors in human immune tissues and leukocyte subpopulations. Eur J Biochem. 1995; 232:54–61. [PubMed: 7556170]
45. Jiang S, Fu Y, Avraham HK. Regulation of hematopoietic stem cell trafficking and mobilization by the endocannabinoid system. Transfusion. 2011; 51(suppl 4):65S–71S. [PubMed: 22074629]
46. Lin H-F, Traver D, Zhu H, et al. Analysis of thrombocyte development in CD41-GFP transgenic zebrafish. Blood. 2005; 106:3803–3810. [PubMed: 16099879]
47. Jin S-W, Beis D, Mitchell T, et al. Cellular and molecular analyses of vascular tube and lumen formation in zebrafish. Development. 2005; 132:5199–5209. [PubMed: 16251212]
48. Kikuchi K, Holdway JE, Major RJ, et al. Retinoic acid production by endocardium and epicardium is an injury response essential for zebrafish heart regeneration. Dev Cell. 2011; 20:397–404. [PubMed: 21397850]
49. Zhu H, Traver D, Davidson AJ, et al. Regulation of the lmo2 promoter during hematopoietic and vascular development in zebrafish. Dev Biol. 2005; 281:256–269. [PubMed: 15893977]
50. Lam EYN, Chau JYM, Kalev-Zylinska ML, et al. Zebrafish runx1 promoter-EGFP transgenics mark discrete sites of definitive blood progenitors. Blood. 2009; 113:1241–1249. [PubMed: 18927441]
51. Traver D, Paw BH, Poss KD, et al. Transplantation and in vivo imaging of multilineage engraftment in zebrafish bloodless mutants. Nat Immunol. 2003; 4:1238–1246. [PubMed: 14608381]
52. North TE, Goessling W, Peeters M, et al. Hematopoietic stem cell development is dependent on blood flow. Cell. 2009; 137:736–748. [PubMed: 19450519]
53. Zhao Y, Yuan Z, Liu Y, et al. Activation of cannabinoid CB2 receptor ameliorates atherosclerosis associated with suppression of adhesion molecules. J Cardiovasc Pharmacol. 2010; 55:292–298. [PubMed: 20075743]
54. Bertrand JY, Chi NC, Santoso B, et al. Haematopoietic stem cells derive directly from aortic endothelium during development. Nature. 2010; 464:108–111. [PubMed: 20154733]
55. Jin H, Xu J, Wen Z. Migratory path of definitive hematopoietic stem/progenitor cells during zebrafish development. Blood. 2007; 109:5208–5214. [PubMed: 17327398]
56. Fowler CJ. NSAIDs: eNdocannabinoid stimulating anti-inflammatory drugs? Trends Pharmacol Sci. 2012; 33:468–473. [PubMed: 22664342]
57. Chen P, Hu S, Yao J, et al. Induction of cyclooxygenase-2 by anandamide in cerebral microvascular endothelium. Microvasc Res. 2005; 69:28–35. [PubMed: 15797258]

58. Eichele K, Ramer R, Hinz B. R(+)-methanandamide-induced apoptosis of human cervical carcinoma cells involves a cyclooxygenase-2-dependent pathway. Pharm Res. 2009; 26:346–355. [PubMed: 19015962]
59. Gardner B, Zhu LX, Sharma S, et al. Methanandamide increases COX-2 expression and tumor growth in murine lung cancer. Faseb J. 2003; 17:2157–2159. [PubMed: 12958151]
60. Hinz B, Ramer R, Eichele K, et al. Up-regulation of cyclooxygenase-2 expression is involved in R(+)-methanandamide-induced apoptotic death of human neuroglioma cells. Mol Pharmacol. 2004; 66:1643–1651. [PubMed: 15361550]
61. Mestre L, Correa F, Docagne F, et al. The synthetic cannabinoid WIN 55,212-2 increases COX-2 expression and PGE2 release in murine brain-derived endothelial cells following Theiler's virus infection. Biochem Pharmacol. 2006; 72:869–880. [PubMed: 16914119]
62. Mitchell MD, Sato TA, Wang A, et al. Cannabinoids stimulate prostaglandin production by human gestational tissues through a tissue- and CB1-receptor-specific mechanism. Am J Physiol Endocrinol Metab. 2008; 294:E352–E3566. [PubMed: 18042663]
63. Ramer R, Weinzierl U, Schwind B, et al. Ceramide is involved in r(+)-methanandamide-induced cyclooxygenase-2 expression in human neuroglioma cells. Mol Pharmacol. 2003; 64:1189–1198. [PubMed: 14573769]
64. Slanina KA, Schweitzer P. Inhibition of cyclooxygenase-2 elicits a CB1-mediated decrease of excitatory transmission in rat CA1 hippocampus. Neuropharmacology. 2005; 49:653–659. [PubMed: 15936781]
65. Grosser T, Yusuff S, Cheskis E, et al. Developmental expression of functional cyclooxygenases in zebrafish. Proc Natl Acad Sci USA. 2002; 99:8418–8423. [PubMed: 12011329]
66. Guzmán M. Cannabinoids: Potential anti-cancer agents. Nat Rev Cancer. 2003; 3:745–755. [PubMed: 14570037]
67. Derocq JM, Ségui M, Marchand J, et al. Cannabinoids enhance human B-cell growth at low nanomolar concentrations. FEBS Lett. 1995; 36:177–182. [PubMed: 7544292]
68. Liu Y-J, Fan H-B, Jin Y, et al. Cannabinoid receptor 2 suppresses leukocyte inflammatory migration by modulating the JNK/c-Jun/Alox5 pathway. J Biol Chem. 2013; 288:13551–13562. [PubMed: 23539630]
69. Ghosh S, Preet A, Groopman JE, et al. Cannabinoid receptor CB2 modulates the CXCL12/CXCR4-mediated chemotaxis of T lymphocytes. Mol Immunol. 2006; 43:2169–2179. [PubMed: 16503355]
70. Adhikary S, Kocieda VP, Yen J-H, et al. Signaling through cannabinoid receptor 2 suppresses murine dendritic cell migration by inhibiting matrix metalloproteinase 9 expression. Blood. 2012; 120:3741–3749. [PubMed: 22972984]
71. Yen J-H, Kocieda VP, Jing H, et al. Prostaglandin E2 induces matrix metalloproteinase 9 expression in dendritic cells through two independent signaling pathways leading to activator protein 1 (AP-1) activation. J Biol Chem. 2011; 286:38913–38923. [PubMed: 21940623]
72. Sun G, Pan J, Liu K, et al. Molecular cloning and expression analysis of P-Selectin from Zebrafish (*Danio rerio*). Int J Mol Sci. 2010; 11:4618–4630. [PubMed: 21151460]
73. Sun G, Pan J, Liu K, et al. Molecular cloning and expression analysis of P-selectin glycoprotein ligand-1 from zebrafish (*Danio rerio*). Fish Physiol Biochem. 2012; 38:555–564. [PubMed: 21755364]
74. Ohta S, Inujima Y, Abe M, et al. Inhibition of P-selectin specific cell adhesion by a low molecular weight, non-carbohydrate compound, KF38789. Inflamm Res. 2001; 50:544–551. [PubMed: 11766994]
75. Clements WK, Traver D. Signalling pathways that control vertebrate haematopoietic stem cell specification. Nat Rev Immunol. 2013; 13:336–348. [PubMed: 23618830]
76. Basu S, Dittel BN. Unraveling the complexities of cannabinoid receptor 2 (CB2) immune regulation in health and disease. Immunol Res. 2011; 51:26–38. [PubMed: 21626285]
77. Lévesque J-P, Helwani FM, Winkler IG. The endosteal “osteoblastic” niche and its role in hematopoietic stem cell homing and mobilization. Leukemia. 2010; 24:1979–1992. [PubMed: 20861913]

78. Rossi FMV, Corbel SY, Merzaban JS, et al. Recruitment of adult thymic progenitors is regulated by P-selectin and its ligand PSGL-1. Nat Immunol. 2005; 6:626–634. [PubMed: 15880112]

79. Sultana DA, Zhang SL, Todd SP, et al. Expression of functional P-selectin glycoprotein ligand 1 on hematopoietic progenitors is developmentally regulated. J Immunol. 2012; 188:4385–4393. [PubMed: 22461691]

80. Bajoghli B, Aghaallaei N, Hess I, et al. Evolution of genetic networks underlying the emergence of thymopoiesis in vertebrates. Cell. 2009; 138:186–197. [PubMed: 19559469]

81. Liu C, Saito F, Liu Z, et al. Coordination between CCR7- and CCR9-mediated chemokine signals in prevascular fetal thymus colonization. Blood. 2006; 108:2531–2539. [PubMed: 16809609]

82. Lombard C, Hegde VL, Nagarkatti M, et al. Perinatal exposure to Δ9-tetrahydrocannabinol triggers profound defects in T cell differentiation and function in fetal and postnatal stages of life, including decreased responsiveness to HIV antigens. J Pharmacol Exp Ther. 2011; 339:607–617. [PubMed: 21831965]

83. Cutler C, Multani P, Robbins D, et al. Prostaglandin-modulated umbilical cord blood hematopoietic stem cell transplantation. Blood. 2013; 122:3074–3081. [PubMed: 23996087]

84. Burt J, Chu M. American Chemical Society—236th National Meeting & Exposition. Compound development for prevalent conditions. IDrugs. 2008; 11:693–695. [PubMed: 18828062]

85. Deusch E, Kress HG, Kraft B, et al. The procoagulatory effects of delta-9-tetrahydrocannabinol in human platelets. Anesth Analg. 2004; 99:1127–30. table of contents. [PubMed: 15385362]

86. Matos I, Bento AF, Marcon R, et al. Preventive and therapeutic oral administration of the pentacyclic triterpene α,β-amyrin ameliorates dextran sulfate sodium-induced colitis in mice: The relevance of cannabinoid system. Mol Immunol. 2013; 54:482–492. [PubMed: 23454360]

87. Shinohara M, Mirakaj V, Serhan CN. Functional metabolomics reveals novel active products in the DHA metabolome. Front Immunol. 2012; 3:81. [PubMed: 22566962]

88. Xu H, Cheng CL, Chen M, et al. Anti-inflammatory property of the cannabinoid receptor-2-selective agonist JWH-133 in a rodent model of autoimmune uveoretinitis. J Leukoc Biol. 2007; 82:532–541. [PubMed: 17537989]

89. Gossens K, Naus S, Corbel SY, et al. Thymic progenitor homing and lymphocyte homeostasis are linked via S1P-controlled expression of thymic P-selectin/CCL25. J Exp Med. 2009; 206:761–778. [PubMed: 19289576]

90. Schwab SR, Pereira JP, Matloubian M, et al. Lymphocyte sequestration through S1P lyase inhibition and disruption of S1P gradients. Science. 2005; 309:1735–1739. [PubMed: 16151014]

91. Juarez JG, Harun N, Thien M, et al. Sphingosine-1-phosphate facilitates trafficking of hematopoietic stem cells and their mobilization by CXCR4 antagonists in mice. Blood. 2012; 119:707–716. [PubMed: 22049516]

92. Mair KM, Robinson E, Kane KA, et al. Interaction between anandamide and sphingosine-1-phosphate in mediating vasorelaxation in rat coronary artery. Br J Pharmacology. 2010; 161:176–192.

93. Galve-Roperh I, Sánchez C, Cortés ML, et al. Anti-tumoral action of cannabinoids: Involvement of sustained ceramide accumulation and extracellular signal-regulated kinase activation. Nat Med. 2000; 6:313–319. [PubMed: 10700234]

94. Gustafsson K, Sander B, Bielawski J, et al. Potentiation of cannabinoid-induced cytotoxicity in mantle cell lymphoma through modulation of ceramide metabolism. Mol Cancer Res. 2009; 7:1086–1098. [PubMed: 19609004]

95. Selley DE, Welch SP, Sim-Selley LJ. Sphingosine lysolipids in the CNS: Endogenous cannabinoid antagonists or a parallel pain modulatory system? Life Sci. 2013; 93:187–193. [PubMed: 23782998]

96. Takizawa H, Boettcher S, Manz MG. Demand-adapted regulation of early hematopoiesis in infection and inflammation. Blood. 2012; 119:2991–3002. [PubMed: 22246037]

97. Li Y, Esain V, Teng L, et al. Inflammatory signaling regulates embryonic hematopoietic stem and progenitor cell production. Genes Dev. 2014; 28:2597–2612. [PubMed: 25395663]

98. Sawamiphak S, Kontarakis Z, Stainier DYR. Interferon gamma signaling positively regulates hematopoietic stem cell emergence. Dev Cell. 2014; 31:640–653. [PubMed: 25490269]

99. Espín-Palazón R, Stachura DL, Campbell CA, et al. Proinflammatory signaling regulates hematopoietic stem cell emergence. Cell. 2014; 159:1070–1085. [PubMed: 25416946]

100. He Q, Zhang C, Wang L, et al. Inflammatory signaling regulates hematopoietic stem and progenitor cell emergence in vertebrates. Blood. 2015; 125:1098–1106. [PubMed: 25540193]

Significance Statement

Hematopoietic (blood) stem and progenitor cells (HSPC) form the foundation of our immune system; the production and maturation of these cells are carefully controlled in the body, beginning during embryogenesis in vertebrates. Here we describe the role of cannabinoid receptor 2 (CNR2) signaling, an inflammatory cascade that promotes adult HSPC survival after injury, as a physiologically relevant modifier of the birth, migration and propagation of embryonic HSPCs. CNR2 activity is utilized to ensure production of adequate HSPC numbers and proper seeding of hematopoietic tissues to facilitate establishment and maintenance of the blood system to provide lifelong immune function.

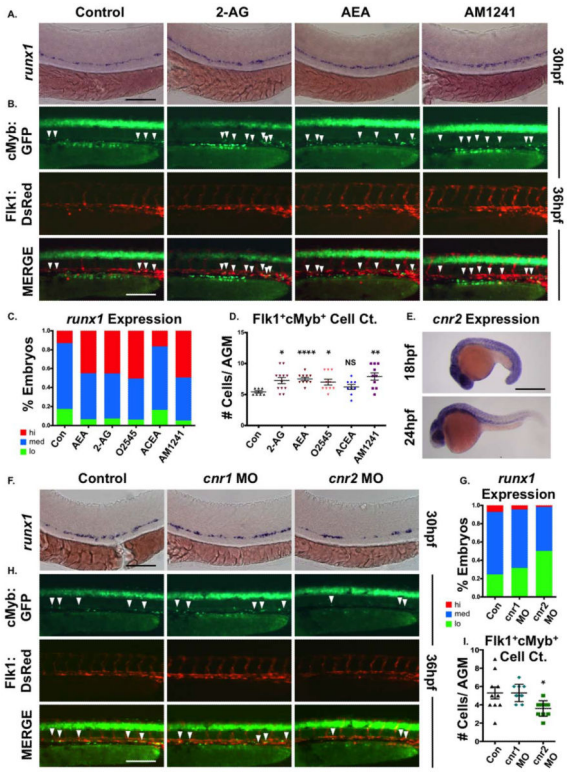

Figure 1.

CNR2 modulates hematopoietic stem cell (HSC) formation during embryogenesis. **(A)**: Embryonic exposure to endogenous (2-AG, 5 μM; AEA, 5 μM) or synthetic (AM1241, CNR2-selective agonist, 10 μM) cannabinoids during HSC formation (12–30 hpf) increased *runx1* expression in the AGM ($n \geq 90$ per condition). **(B)**: In vivo imaging of *flk1:dsRed;cmyb:egfp* embryos indicated the number of Flk1:dsRed^{+};cMyb:GFP^{+} HSCs (arrowheads) was increased in the AGM at 36 hpf following exposure to endogenous and synthetic cannabinoid compounds ($n \geq 7$ per condition). **(C)**: Qualitative phenotypic distribution of embryos from panel (A) and Supporting Information Figure S1A scored with low, medium, or high *runx1* expression in the AGM (O2545: dual CNR1/2 agonist, 5 μM, ACEA: CNR1-selective agonist, 5 μM). **(D)**: Absolute counts of Flk1:dsRed^{+}cMyb:GFP^{+} HSCs in embryos from panel (B) and Supporting Information Figure S1B (DMSO: 5.4±0.5, 2-AG: 7.3±1.7, AEA: 7.5±2.4, O2545: 7±1.5, ACEA: 6.2±1.2, AM1241: 7.9±1.9; *, $p \leq .05$; **, $p \leq .01$; ****, $p \leq .0001$, two-tailed *t* test). **(E)**: Whole-mount in situ hybridization of wild type embryos at 18 and 24 hpf showed *cnr2* was expressed throughout the embryo and enriched in the AGM region at the time of HSC specification. **(F)**: MO-mediated knockdown of *cnr1* or *cnr2* revealed that CNR2, but not CNR1, was required for normal *runx1* expression ($n \leq 150$ per condition). **(G)**: Qualitative phenotypic distribution of embryos from panel (F) scored with low, medium, or high *runx1* expression in the AGM. **(H)**: In vivo imaging confirming the number of Flk1:dsRed^{+};cMyb:GFP^{+} HSCs (arrowheads) was decreased in the AGM at 36 hpf following *cnr2*, but not *cnr1*, MO-mediated knockdown ($n \geq 10$ per condition). **(I)**: Absolute counts of Flk1:dsRed^{+}cMyb:GFP^{+} HSCs from embryos in panel (B) (uninjected: 5.3±0.7, *cnr1* MO: 5.3±0.3, *cnr2* MO: 3.6±0.3; *, $p < .05$, two-tailed

t test). Scale bars: (A, B, F, H)=100 μm, (E) =500 μm. Abbreviations: 2AG, 2-arachidonoylglycerol; AEA, anandamide; AGM, aorta-gonad-mesonephros; MO, morpholino.

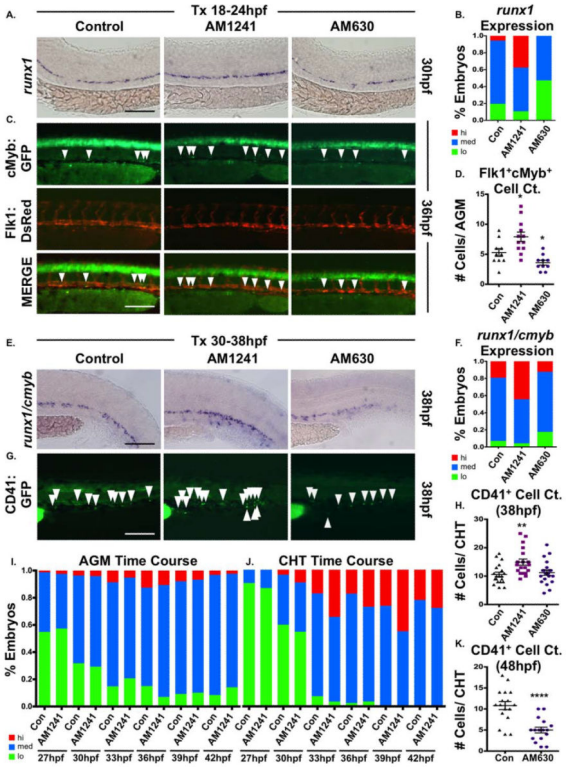

Figure 2.

CNR2 modulation impacts hematopoietic stem cell (HSC) development in the AGM and CHT. **(A)**: Embryos exposed to AM1241 or AM630 (CNR2-selective antagonist, 10 μM each) during niche specification (18–24 hpf) exhibited increased or decreased *runx1* expression in the AGM at 30 hpf, respectively ($n \geq 55$ per condition). **(B)**: Qualitative phenotypic distribution of embryos from panel (A), scored with low, medium, or high *runx1* expression in the AGM. **(C)**: In vivo imaging confirmed the number of Flk1:dsRed^{+};cMyb:GFP^{+} HSCs (arrowheads) in the AGM was altered at 36 hpf following exposure (18–24 hpf) to AM1241 or AM630 ($n \geq 10$ per condition). **(D)**: Absolute counts of Flk1:dsRed^{+}cMyb:GFP^{+} HSCs from embryos in panel (C) (DMSO: 5.3±0.7, AM1241: 7.9±0.8, AM630: 3.6±0.4; *, $p \leq .05$, two-tailed *t* test). **(E)**: Embryos exposed to CNR-modifiers during the phase of HSC production (30–38 hpf) exhibited altered *runx1;cmyb*$^{+}$ expression in the CHT (scored as the vascular region beyond the tip of the yolk sac extension) at 38 hpf ($n \geq 55$ per condition). **(F)**: Qualitative phenotypic distribution of embryos from panel (E), scored with low, medium, or high *runx1;cmyb* expression in the CHT. **(G)**: In vivo imaging of *cd41:egfp* embryos indicated the number of CD41^{+} HSCs (arrowheads) was increased in the CHT at 38 hpf following exposure to AM1241 but not significantly altered in embryos exposed to AM630 ($n \geq 20$ per condition). **(H)**: Absolute counts of CD41:GFP^{+} cells from embryos in panel (G) (DMSO: 10.6±0.8, AM1241: 15.0±1.1, AM630: 11.3±0.9; **, $p \leq .01$, two-tailed *t* test). **(I)**: Time course analysis of the qualitative phenotypic distribution of *runx1;cmyb* expression in the AGM region of embryos exposed to AM1241 during the phase of HSC production (24 hpf until time indicated) ($n \geq 55$ per condition). **(J)**: Time course analysis of the qualitative phenotypic distribution of

runx1;cmyb expression in the CHT region as described for panel (I), showing increased colonization in response to AM1241 compared to wild type sibling controls (see also Supporting Information Fig. S2E). **(K)**: Embryos exposed to AM630 during HSC production (30–48 hpf) had decreased numbers of $CD41^{+}$ HSCs at 48 hpf (DMSO: 11.6±0.6, AM630: 7.2±0.6; ****, $p \leq .0001$, two-tailed *t* test; see also Supporting Information Fig. S2F). Scale bars (A, C, E, G)=100 μm. Abbreviations: AGM, aorta-gonad-mesonephros; CHT, caudal hematopoietic tissue.

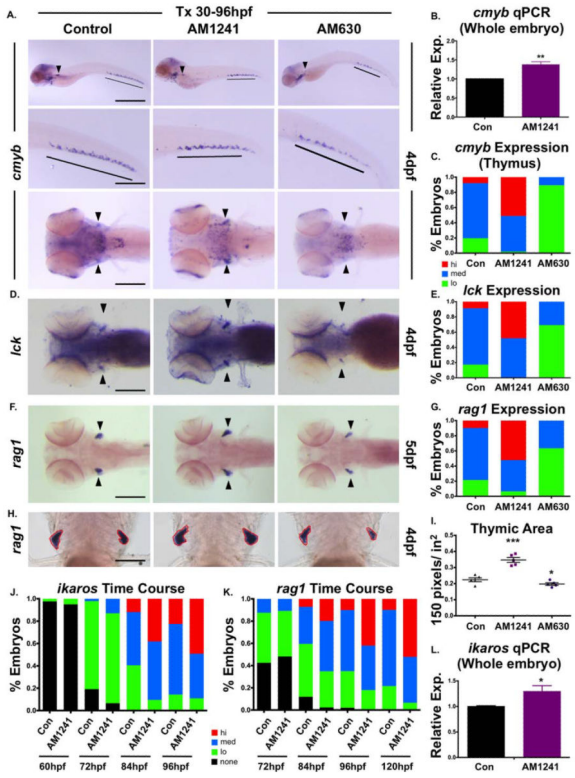

Figure 3.

CNR2 modulation impacts hematopoietic stem and progenitor cell colonization of thymus. **(A)**: Exposure to CNR2-modulators (30–96 hpf) during the window of hematopoietic stem cell (HSC) expansion and secondary niche colonization affected *cmyb*$^{+}$ expression (upper row, lateral view; line, caudal hematopoietic tissue (CHT) region; arrowhead, kidney marrow; middle row, close up of CHT; lower row, dorsal view; arrowheads, thymi) with AM1241 increasing thymic colonization, and AM630 decreasing expression in all hematopoietic sites (n>45 per condition). **(B)**: qPCR analysis indicated AM1241-treatment (30–96 hpf) increased total *cmyb* expression at 4 dpf (n=4, AM1241: 1.38±0.07-fold; $p \leq .01$, two-tailed t test). **(C)**: Qualitative phenotypic distribution of low, medium, or high thymic *cmyb* expression from embryos exposed to AM1241 and AM630 (30–96 hpf) as in panel (A). **(D)**: Embryos exposed to AM1241 and AM630 during HSC expansion as in panel (A) showed an altered thymic expression of *lck* (n>20 per condition). **(E)**: Qualitative phenotypic distribution of embryos from panel (D), scored with low, medium, or high *lck* expression in the thymus. **(F)**: Embryos exposed to AM1241 and AM630 as in panel (A) showed increased or decreased thymic expression of *rag1*, respectively (n>45 per condition). **(G)**: Qualitative phenotypic distribution of embryos from panel (F), scored with low, medium, or high *rag1* expression in the thymus. **(H)**: Representative examples of total thymic area measurements (outlined in red) in AM1241- or AM630-exposed embryos (30–96 hpf) following *rag1* whole mount in situ hybridization. **(I)**: Bar graph of total thymic area from panel (H) (DMSO: 0.224±0.012 a.u., AM1241: 0.347±0.015, AM630: 0.197±0.008; *, $p \leq .05$; ***, $p \leq .001$, one-tailed t test, n=5). **(J)**: Time course analysis (60–96 hpf) of the qualitative phenotypic distribution of *ikaros* expression in the thymus as described for panel

(A), showing increased colonization in response to AM1241 compared to wild type sibling controls ($n \geq 40$). **(K)**: Time course analysis (72–120 hpf) of the qualitative phenotypic distribution of *rag1* expression in the thymus as described for panel (A), indicating increased lymphoid commitment in response to AM1241 compared to controls ($n \geq 40$). **(L)**: qPCR confirmation of increase *ikaros* expression at 4 dpf in embryos exposed to AM1241 during HSC expansion and niche colonization (30–96 hpf) (AM1241: 1.30±0.11-fold, $p \geq .05$; *, $p \leq .05$, two-tailed *t* test, $n=3$). Scale bars (A, top)=800 μm, (A, middle)=400 μm, (A, bottom), (D, F)=200 μm, (H)=100 μm. Abbreviation: qPCR, quantitative polymerase chain reaction.

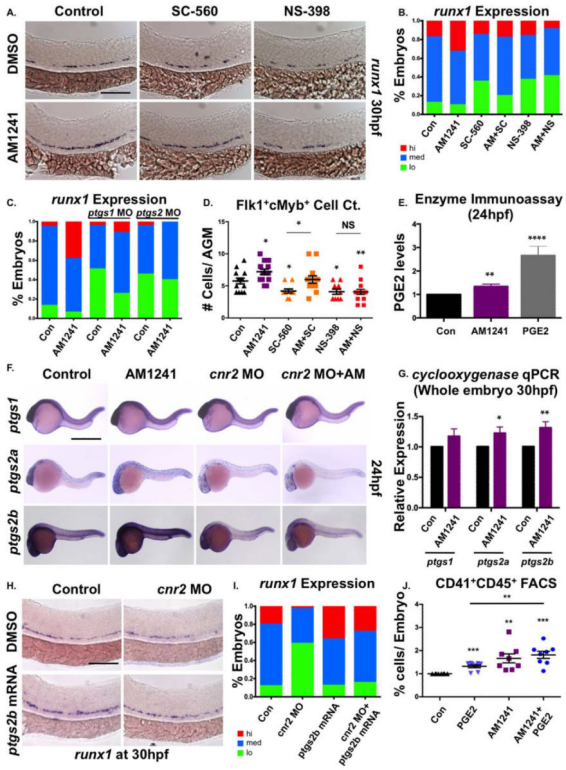

Figure 4.

CNR2-signaling increases PGE2 production via *ptgs2* induction. **(A)**: Treatment with selective cyclooxygenase (Ptgs)-1 (SC-560, 10 μM) and Ptgs2 (NS-398, 10 μM) inhibitors (12–30 hpf) decreased *runx1* expression in the AGM; the effect of SC-560 on *runx1*, but not that of NS-398, was ameliorated by addition of AM1241 (*n*≥90 per condition). **(B)**: Qualitative phenotypic distribution of embryos from panel (A), scored with low, medium, or high *runx1* expression in the AGM. **(C)**: Qualitative phenotypic distribution of embryos injected with *ptgs1* or *ptgs2a*/*ptgs2b* MOs in the presence or absence of AM1241-treatment, scored with low, medium, or high *runx1* expression; the effect of MO-mediated reduction in Ptgs1, but not that of Ptgs2, on *runx1* was restored to wild type levels by exposure to AM1241 (*n*≥25 per condition). **(D)**: Quantification of the independent and combined effects of selective Ptgs inhibitors and AM1241 by absolute counts of Flk1:dsRed^{+};cMyb:GFP^{+} hematopoietic stem cells in embryos, treated as in panel (A), indicated AM1241 acts via Ptgs2 to impact HSCs (DMSO: 5.8±0.5, AM1241: 7.2±0.4, SC-560, 4.1±0.4, AM1241+SC-560: 6.0±0.6, NS-398: 05.8±0.5, AM1241+NS-398: 04.1±0.4; *, $p \leq .05$, two-tailed *t* test, *n*≥10 per condition). **(E)**: Embryos exposed to AM1241 (12–24 hpf) exhibited augmented PGE2 production: relative concentration of PGE2 was measured in AM1241- and PGE2-treated (positive control) embryos via a biochemical assay for PGE2-metabolites (PGE2, 2.66-fold; AM1241, 1.35-fold; **, $p<.01$, two-tailed *t* test, *n*=7). **(F)**: Whole-mount in situ hybridization for *ptgs1*, *ptgs2a*, and *ptgs2b* at 24 hpf showed each was upregulated in response to AM1241 exposure (12–24 hpf); MO knockdown of *cnr2* decreased the expression level of *ptgs2a* and *ptgs2b*, but not of that of *ptgs1*, and blocked the transcriptional response to AM1241-treatment (*n*≥25 per condition). **(G)**: qPCR analysis at

30 hpf confirmed *ptgs2a* and *ptgs2b* were significantly upregulated over baseline following AM1241 exposure, whereas *ptgs1* expression was not (*ptgs1*: 1.17-fold, NS; *ptgs2a*: 1.22-fold, *, $p<.05$; *ptgs2b*: 1.31-fold, **, $p\leq.01$, two-tailed *t* test, $n=25$ pooled embryos per condition × >10 replicates). **(H)**: Overexpression of *ptgs2b* normalized *runx1* expression in the AGM of *cnr2* morphants ($n\geq40$ per condition). **(I)**: Qualitative phenotypic distribution of embryos from panel (I), scored with low, medium, or high *runx1* expression in the AGM. **(J)**: The effect of combinatorial AM1241- and dmPGE2-treatment (5 μM each) was quantified by FACS using *cd41:gfp*;*cd45:dsRed* embryos (dmPGE2: 1.32-fold, AM1241: 1.66-fold, AM1241+dmPGE2: 1.82-fold; **, $p\leq.01$; ***, $p\leq.001$, two-tailed *t* test, $n=8$ per condition). Scale bars (A)=100 μm, (F)=800 μm, (H)=125 μm. Abbreviations: AGM, aorta-gonad-mesonephros; DMSO, Dimethyl Sulfoxide; FACS, fluorescence-activated cell sorting; MO, morpholino; PGE2, prostaglandin E2; ptgs, prostaglandin endoperoxide synthase; qPCR, quantitative polymerase chain reaction.

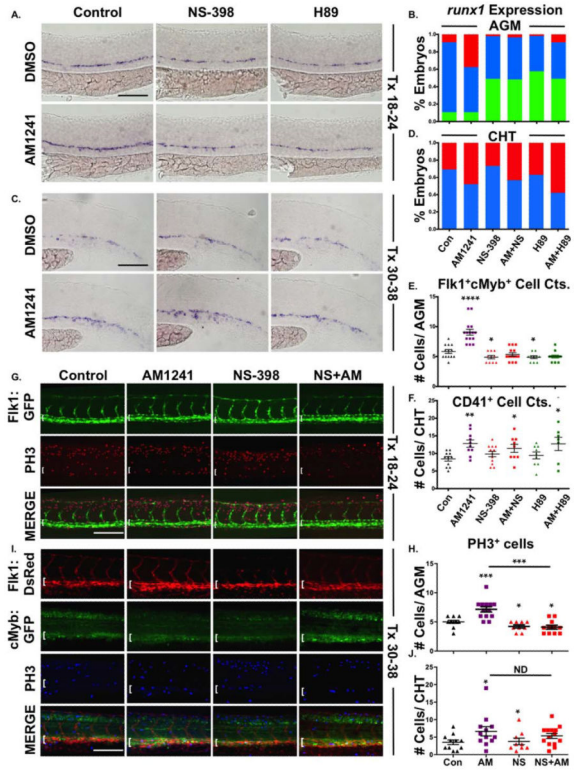

Figure 5.

AM1241 mediates hematopoietic stem cell (HSC) expansion in the AGM, but not CHT, via PGE2-signaling. **(A)**: Treatment with selective inhibitors to Ptgs2 (NS-398) or PKA/cAMP (H89, 5 μM) during niche specification (18–24 hpf) decreased *runx1* expression and blocked AM1241-mediated inductions in hematopoietic stem and progenitor cell (HSPC) expression in the AGM ($n \geq 45$ per condition).**(B)**: Qualitative phenotypic distribution of embryos from panel (A), scored with low, medium, or high *runx1* expression in the AGM. **(C)**: Treatment with NS-398 or H89 during hematopoietic stem cell (HSC) production (30–38 hpf) failed to block AM1241-mediated elevations in *runx1;cmyb* expression in the CHT ($n \geq 75$ per condition). **(D)**: Qualitative phenotypic distribution of embryos from panel (C), scored with low, medium, or high *runx1* expression in the CHT. **(E)**: Absolute counts of Flk1:dsRed^{+};cMyb:GFP^{+} HSCs confirmed PGE2 production and signaling are required to mediate the effects of AM1241 in the AGM (DMSO: 5.8±0.3, AM1241: 9.1±0.5, NS-398: 4.9±0.3, AM1241+NS-398: 5.4±0.3, H89: 4.9±0.2, AM1241+NS-398: 5.0±0.2; *, $p \leq .05$; ****, $p < .0001$, two-tailed *t* test, $n \geq 10$ per condition). **(F)**: Absolute counts of CD41:GFP^{+} HSCs confirmed AM1241-mediated increases in the CHT are independent of PGE2 production and signaling (DMSO: 8.5±0.6, AM1241: 12.8±1, NS-398: 9.8±0.8, AM1241+NS-398: 11.4±1.1, H89: 9.4±1.0, AM1241+NS-398: 12.7±1.9, *, $p \leq .05$; **, $p \leq .01$, two-tailed *t* test, n≥9 per condition). **(G)**: Embryos exposed to AM1241 during niche specification (18–24 hpf) exhibited an increased number of pH3^{+} (red) cells in the Flk1:GFP^{+} hemogenic vasculature of the AGM (dorsal aorta marked with white bracket) at 30 hpf, which was blocked by cotreatment with NS-398 ($n \geq 9$ per condition). **(H)**: Absolute counts of pH3^{+} cells in the AGM, as described in panel (G) (DMSO: 5.0±0.27, NS-398:

4.22±0.28, AM1241: 7.15±0.45, AM1241+NS-398: 4.09±0.34; *, $p \leq .05$; ***, $p \leq .001$, two-tailed *t* test). **(I)**: Embryos exposed to AM1241 during HSC production (30–38 hpf) exhibited a higher number of $pH3^+$ (blue) cMyb:GFP^+ HSPCs in the Flk1:dsRed vasculature of the CHT (CHT width marked with white bracket) at 38 hpf; this effect was independent of Ptgs2 activity ($n \geq 9$ per condition). **(J)**: Absolute counts of cMyb:GFP^+;$pH3^+$ cells in the CHT, as described in panel (I) (DMSO: 3.55±0.57, NS-398: 3.78±0.94, AM1241: 6.67±1.33, AM1241+NS-398: 5.36±0.72; *, $p < .05$, two-tailed *t* test). Scale bars (A, C)=80 μm, (G, I)=100 μm. Abbreviations: AGM, aorta-gonad-mesonephros; CHT, caudal hematopoietic tissue; DMSO, Dimethyl Sulfoxide; GFP, green fluorescent protein; PH3, phospho-histone 3.

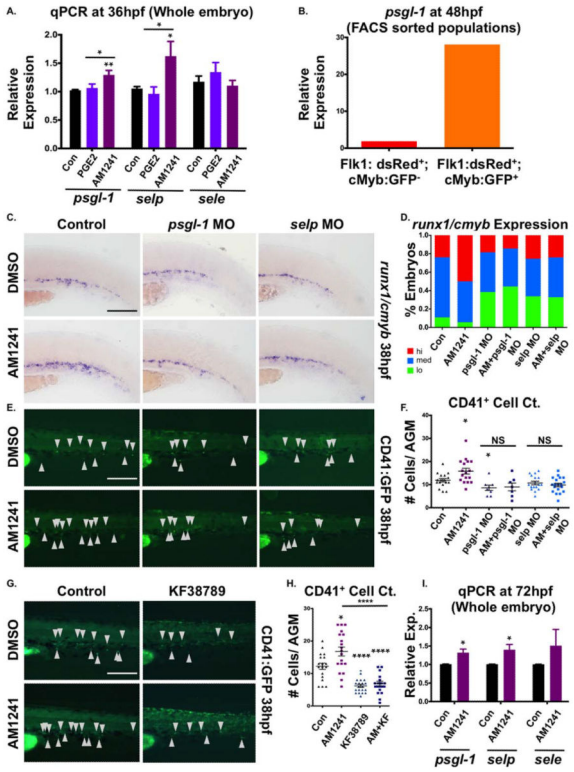

Figure 6.

P-selectin mediates the effect of CNR2-stimulation in the caudal hematopoietic tissue (CHT). **(A)**: qPCR analysis revealed expression of *p-selectin* (*selp*) and its ligand (*psgl-1*) were significantly upregulated by AM1241- but not PGE2-exposure (30–36 hpf) (*psgl-1*: dmPGE2, 1.06-fold; AM1241, 1.29-fold; *selp*: dmPGE2, 0.96-fold; AM1241, 1.62-fold; *sele*: dmPGE2, 1.34-fold; AM1241, 1.10-fold; *, $p \leq .05$; **, $p \leq .01$, two-tailed *t* test, $n \geq 7$). **(B)**: qPCR analysis using FACS-sorted populations from *flk1:dsRed*;*cmyb:GFP* embryos at48 hpf showed that *psgl-1* is expressed at a higher level in HSCs (Flk1:dsRed$^+$;cMyb:GFP$^+$: 28.1 a.u.) than in the vasculature (Flk1:dsRed$^+$; cMyb:GFP$^-$: 1.86 a.u.) (normalized to *18s*). **(C)**: Knockdown of *psgl-1* and *selp* by MO injection reduced *runx1*;*cmyb* expression in the CHT and inhibited the effect of AM1241 (30–38 hpf) on hematopoietic stem and progenitor cell production ($n \geq 60$ per condition). **(D)**: Qualitative phenotypic distribution of embryos from panel (C), scored with low, medium, or high *runx1;cmyb* expression in the CHT at 38 hpf. **(E)**: In vivo imaging of *cd41:egfp* embryos showed that P-selectin knockdown decreased the number of CD41:GFP$^+$ HSCs in the CHT (arrowheads) at 38 hpf and prevented AM1241-stimulated expansion ($n \geq 7$ per condition). **(F)**: Absolute counts of CD41:GFP$^+$ cells confirmed P-selectin activity was required for increased hematopoietic stem cell (HSCs) numbers in the CHT mediated by AM1241 (control/DMSO: 11.9±0.7, *psgl-1* MO/DMSO: 8.6±1.1, *selp* MO/DMSO: 9.9±0.7 control/AM1241: 15.8±1.2, *psgl-1* MO/AM1241: 9.0±1.7, *selp* MO/AM1241: 10.7±0.8; *, $p \leq .05$, two-tailed *t* test). **(G)**: Exposure (30–38 hpf) to a selective inhibitor of P-selectin-mediated cell adhesion (KF38789, 0.5 μM) confirmed the requirement of P-selectin activity for normal and AM1241-enhanced CD41:GFP$^+$ HSC numbers in the CHT ($n \geq 18$). **(H)**:

Absolute counts of CD41:GFP^{+} HSCs in the CHT after exposure to KF38789 and/or AM1241 (DMSO: 12.2±1.0, AM1241: 16.8±1.4, KF38789: 6.2±0.5, AM1241+KF38789: 6.9±0.7; *, $p \leq .05$; ****, $p \leq .0001$, two-tailed *t* test). **(I)**: qPCR analysis showed that expression of *selp* and *psgl-1* was significantly upregulated during HSC expansion and secondary niche colonization (30–72 hpf) (*psgl-1*: 1.31-fold; *selp*: 1.40-fold; *sele*: 1.51-fold; *, $p \leq .05$, two-tailed *t* test, $n=4$ replicates). Scale bars (C, E, G)=100 μm. Abbreviations: DMSO, Dimethyl Sulfoxide; FACS, fluorescence-activated cell sorting; MO, morpholino;PGE2, prostaglandin E2; *psgl-1*, *p-selectin glycoprotein ligand-1*; qPCR, quantitative polymerase chain reaction; *selp*, *p-selectin*; *sele*, *e-selectin*.

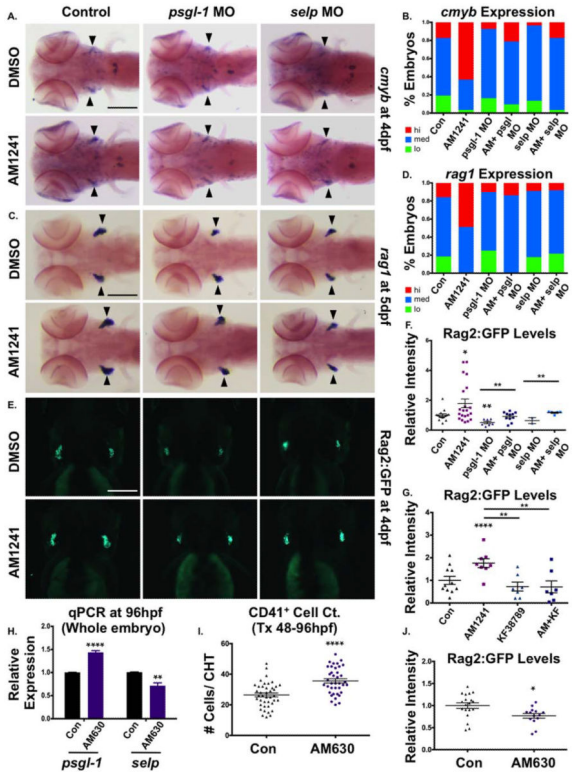

Figure 7.

CNR2-signaling promotes thymic colonization via P-selectin activity. **(A)**: MO-mediated knockdown of *psgl-1* and *selp* reduced *cmyb* expression in the thymus and prevented AM1241 (30–96 hpf) from increasing thymic colonization ($n \geq 50$ per condition). **(B)**: Qualitative phenotypic distribution of embryos from panel (A), scored with low, medium, or high *cmyb* expression in the thymus at 96 hpf. **(C)**: MO-mediated knockdown of *psgl-1* and *selp*, as described in panel (A), decreased *rag1* expression in the thymus in the presence and absence of AM1241 (30–120 hpf) ($n \geq 35$ per condition). **(D)**: Qualitative phenotypic distribution of embryos from panel (C), scored with low, medium, or high *rag1* expression in the thymus at 96 hpf. **(E)**: In vivo imaging of *rag2:egfp* embryos confirmed that *psgl-1*- and *selp*-MOs decreased the number of Rag2:GFP$^+$ lymphoid progenitors in the thymus both with and without AM1241-treatment ($n \geq 8$ per condition). **(F)**: Relative fluorescent intensity of the thymus in morphant embryos, as described in panel (E) (control/DMSO: 1.00±0.10 a.u., *psgl-1* MO/DMSO:0.51±0.08, *selp* MO/DMSO: 0.64±0.29, Control/AM1241: 1.79±0.29 a.u., *psgl-1* MO/AM1241: 0.91±0.09, *selp* MO/AM1241: 1.17±0.53; *, $p \leq .05$; **, $p \leq .01$, one-tailed *t* test). **(G)**: Exposure to KF38789 (30–96 hpf) confirmed the role of P-selectin in normal and AM1241-enhanced thymic colonization, as indicated by Rag2:GFP at 96 hpf (DMSO: 1.00±0.18 a.u., AM1241: 1.76±0.20, KF38789: 0.73±0.20, AM1241+KF38789: 0.71±0.26; **, $p \leq .01$; ****, $p \leq .0001$, two-tailed *t* test, $n \geq 7$ per condition). **(H)**: qPCR analysis showed that exposure to AM630 after the phase of HSC induction (48–96 hpf) altered the expression of *psgl-1* and *selp* (*psgl-1*: 1.44-fold, *selp*: 0.72-fold, **, $p \leq .01$; ****, $p \leq .0001$, two-tailed *t* test). **(I)**: Absolute counts of CD41:GFP$^+$ cells revealed that exposure to AM630, as described in panel (H), increased the number of HSCs

remaining in the CHT at 96 hpf (DMSO: 26.4±1.3, AM630: 35.6±1.4; ****, $p \leq .0001$, two-tailed *t* test, $n \geq 38$,). **(J)**: Relative fluorescent intensity of Rag2:GFP^+ cells the thymus following exposure to AM630, as described in panel (G), indicated CNR2-signaling was required for thymic colonization (DMSO: 1.0±0.06 a.u., AM630: 0.77±0.05 a.u.; *, $p \leq .05$, two-tailed *t* test, $n \geq 14$). Scale bars (A, C)=200 μm, (E)=175 μm. Abbreviations: DMSO, dimethyl sulfoxide; GFP, green fluorescent protein; MO, morpholino; *psgl-1*, *p-selectin glycoprotein ligand-1*; qPCR, quantitative polymerase chain reaction; *sele*, *e-selectin*.